Supplement to:

Accumbal Histamine Signaling Engages Discrete Interneuron Microcircuits

Supplemental Methods and Materials

Animals

Animals were bred and housed at Vanderbilt University Medical Center in accordance with Institutional Animal Care and Use Committees. Male mice on a C57BL/6J background 7-12 weeks of age were used for all electrophysiological experiments. Experimental mice were housed in groups of 3-5/cage on a 12-hr light-dark cycle with *ad libitum* access to food and water. Breeding cages were given 5LOD chow to improve litter viability. For all electrophysiological experiments examining PV-INs, Cre-induced STOP$^{fl/fl}$-tdTomato mice (Ai9, *Gt(ROSA)26Sor*$^{tm9(CAG\text{-}tdTomato)Hze}$) obtained from The Jackson Laboratory (Stock No.: 007909) were crossed with parvalbumin (PV) PV-IRES-Cre mice (PV^{Cre}, *Pvalb*$^{tm1(cre)Arbr/J}$, Stock No.: 012358), generating PV^{Cre}-tdTomato$^{fl/fl}$ (PV^{tdT}) mice. For experiments examining CINs, STOP$^{fl/fl}$-tdTomato (Ai9) mice were crossed with choline acetyltransferase (ChAT) ChAT-IRES-Cre mice (ChAT^{Cre}, *Chat*$^{tm2(cre)Lowl}$, Stock No.: 031661), generating ChAT^{Cre}-tdTomato$^{fl/fl}$ (ChAT^{tdT}) mice. Experiments requiring optogenetic access to the prefrontal cortex (PFC) or mediodorsal thalamus (MDT) were performed in C57BL/6J wild-type (WT) and PV^{Cre} mice.

Slice preparation

Patch-clamp electrophysiological recordings were obtained in acute brain slice preparations from PV^{tdT}, ChAT^{tdT}, or WT mice. Mice were euthanized under isoflurane anesthesia after which

parasagittal slices (250 μM) containing the medial NAc shell (NAcSh) were prepared from whole brain tissue using a Leica Vibratome in oxygenated (95% O2; 5% CO2) ice-cold *N*-methyl-*D*-glucamine (NMDG)-based solution (in mM: 2.5 KCl, 20 HEPES, 1.2 NaH_2PO_4, 25 Glucose, 93 NMDG, 30 $NaHCO_3$, 5.0 sodium ascorbate, 3.0 sodium pyruvate, 10 $MgCl_2$, and 0.5 $CaCl_2$-$2H_2O$). Slices were then recovered in NMDG-based recovery solution for 10-15-min at 30-32 °C before being transferred to a chamber containing artificial cerebral spinal fluid (ACSF, in mM: 119 NaCl, 2.5 KCl, 1.3 $MgCl_2$-$6H_2O$, 2.5 $CaCl_2$-$2H_2O$, 1.0 NaH_2PO4-H_2O, 26.2 $NaHCO_3$, and 11 glucose; 287-295 mOsm).

All experiments were performed using a Scientifica Slicescope Pro System with continuously-perfused 28-32°C ACSF at 2 mL/min. PV-INs and CINs in the NAcSh were visualized using Scientifica PatchVision software and differentiated according to the expression of the tdTomato fluorophore via 530 nm LED light. PV-INs were confirmed according to biophysical properties (capacitance, membrane resistance, AMPAR decay kinetics, and fast-spiking action potential profile) and patched with 3–7 MΩ recording pipettes (P1000 Micropipette Puller). CINs were confirmed according to morphological properties (size, shape) and cellular properties (hyperpolarization-activated voltage sag, spontaneous and accommodating action potential firing).

Whole-cell recordings were performed in a K^+-based intracellular solution: (in mM: 135 K^+-gluconate, 5 NaCl, 2 $MgCl_2$, 10 HEPES, 0.6 EGTA, 3 Na_2ATP, 0.4 Na_2GTP; 285-292 mOsm). Experiments requiring a depolarized command voltage to isolate GABAergic transmission were performed in a Cs^+-based intracellular solution: (in mM: 120 $CsMeSO_3$, 15 CsCl, 8 NaCl, 10 HEPES, 0.2 EGTA, 10 TEA-Cl, 4.0 Mg-ATP, 0.3 Na-GTP, 0.1 spermine, and 5.0 QX 314

bromide). GABAergic transmission recorded at -70 mV was performed in a symmetrical chloride internal solution (in mM: 120 CsCl, 15 CsCl, 8 NaCl, 10 HEPES, 0.2 EGTA, 10 TEA-Cl, 4.0 Mg-ATP, 0.3 Na-GTP, 0.1 spermine, and 5.0 QX314 bromide) and isolated with AMPAR antagonist, NBQX, and NMDAR antagonist, APV. Cell-attached recordings were performed with 5-7 MΩ recording pipettes backfilled with ACSF. For voltage-clamp recordings of glutamatergic transmission, AMPAR-mediated electrically-evoked excitatory postsynaptic currents (EPSCs) were obtained at -70 mV and isolated with $GABA_AR$ antagonist, picrotoxin. Optically-evoked inhibitory postsynaptic currents ($oIPSC^{FFI}$) in MSNs were isolated electrochemically at 0 mV using the E_{Cl} and $E_{AMPAR/NMDAR}$ of the Cs^+-based internal solution. In experiments examining local synaptic transmission, a bipolar electrode was placed at the corticoaccumbens interface and stimulated at 0.1 Hz. Paired pulse ratios (PPR) were obtained within-experiment by delivering two 0.3-ms duration pulses with a 50-ms interstimulus interval and calculating the amplitude ratio of the second EPSC to the first EPSC ($EPSC_2/EPSC_1$). In optogenetic experiments examining input-specific synaptic transmission, 473-nm Cool LED stimulation was delivered at 0.1 Hz with a 0.3-1-ms pulse duration.

Membrane resistance (R_m) and series resistance (R_S) were monitored continuously during all experiments, with >15% change in R_S resulting in the omission of that experiment. Postsynaptic conductances were quantified according to time-locked changes in holding current ($I_{holding}$) and membrane resistance obtained within experiment in voltage-clamp configuration. To measure SK channel-mediated medium afterhyperpolarizations (mAHPs), CINs were voltage-clamped at –60 mV followed by a 200-ms voltage-step to +10 mV. The maximum mAHP tail-current (I_{Tail}) was measured within 200-ms following the voltage step and confirmed with SK channel blocker,

apamin. For current-clamp recordings, cells were permitted 5-min after entering whole-cell configuration to equilibrate to the intracellular dialysate, after which a depolarizing plateau potential was established to maintain cells at -70 mV. The mAHP amplitude of CINs was quantified at resting membrane potential as the peak AHP relative to threshold. To assess intrinsic membrane excitability, action potentials (APs) were elicited following 50 pA current steps increasing from -400 to 550 pA with an 800-ms step duration every 2-min. Input-output experiments exhibiting depolarization block were omitted from analysis. The maximum hyperpolarized-activated voltage sag (V_{SAG}) was measured following somatic current injection of -200 and -400 pA. Cell-attached recordings of sAPs in CINs were recorded following a 5-min stabilization period, after which sAP firing frequency was averaged over 1-min intervals.

Voltammetry

Ex vivo fast-scan cyclic voltammetry (FSCV) was used to characterize dopamine release and the pharmacodynamic properties of a variety of pharmacological combinations at dopamine terminals in the medial NAcSh. A vibrating tissue slicer was used to prepare 300 µm-thick coronal brain sections containing the NAc, which were immersed in oxygenated ACSF containing (in mM): NaCl (126), KCl (2.5), NaH_2PO_4 (1.2), CaCl2 (2.4), $MgCl_2$ (1.2), $NaHCO_3$ (25), glucose (11), L-ascorbic acid (0.4) and pH was adjusted to 7.4. The slice was transferred to the recording chambers containing ACSF at 32 °C with a 1 mL/min flow rate. A carbon fiber microelectrode (100–200 µm length, 7 µm radius) and bipolar stimulating electrode were placed into the NAcSh. A carbon fiber microelectrode (100–200 µm length, 7 µm radius) and bipolar stimulating electrode were placed in close proximity into the NAcSh. Tonic dopamine release was evoked by a single electrical pulse

(350 μA, 4-ms, monophasic) applied to the tissue every 3-min. Tonic firing was mimicked by stimulations that consisted of single electrical stimulations, selected based on the tonic physiological firing properties of VTA dopamine neurons *in vivo*. The extracellular dopamine level was recorded by applying a triangular waveform (-0.4 to +1.2 to -0.4 V vs Ag/AgCl, 400 V/s). Once the peak of electrically-evoked dopamine release stabilized (3 collections with <10% variability), the amount of evoked dopamine release was assessed. Recording electrodes were calibrated by recording responses (in electrical current; nA) to a known concentration of dopamine (3 μM) using a flow-injection system, enabling the conversion of an electrical current (nA) to a known dopamine concentration (μM).

Stereotaxic surgery

6–8-week-old male WT or PV^{tdT} mice were anesthetized using ketamine (75 mg/kg I.P.) and Dexdomitor (0.5 mg/kg I.P.). Craniotomies were performed using a drill, AmScope microscope, and World Precision Instruments Aladdin Al-2000 syringe pump hydraulic system. The following coordinates were used based on The Mouse Brain in Stereotaxic Coordinates: PFC (AP 1.4, ML ± 0.5, DV −2.9 mm) and MDT (AP −1.2, ML 0.3, DV −3.00 mm). Injection sites were located using Leica AngleTwo Stereotaxic software. AAV-CaMKII-ChR2-eYFP (Addgene) was injected at 100 nL/min. Mice were revived using antisedan (atipamezole, 0.5 mg/kg I.P.) and treated with ketoprofen (5 mg/kg I.P.) for 3 days post-operatively. ChR2 expression and anatomical specificity were validated empirically according to the expression of eYFP in the medial PFC or paraventricular region of the MDT and high-fidelity AMPAR-mediated optically-evoked EPSCs (oEPSCs) with rapid decay kinetics in NAc PV(+)-INs.

Pharmacology

Histamine dihydrochloride, NBQX disodium salt, APV, thioperamide, JNJ 5207852, dimaprit, cetirizine, ZD7288, ranitidine, 2-pyridylethylamine, *R*-(-)-α-methyl-histamine, apamin, forskolin, H89, dibutyryl cAMP, BAPTA-AM, ω-conotoxin GVIA, ω-agatoxin TK, dihydro-β-erythroidine, and scopolamine were purchased from Tocris Bioscience. Picrotoxin was purchased from Sigma Aldrich. H_3R antagonists, thioperamide and JNJ5207852, were used interchangeably with equal efficacy, as described in Manz et al., 2020a.

Statistics and Data Analysis

Electrophysiological experiments were analyzed using Clampfit 10.4 and GraphPad Prism v8.4 (GraphPad Software, San Diego, CA). DEMON voltammetry and analysis software were used for all analysis of FSCV data. Data were modeled via analysis of peak and decay kinetics to determine the peak. Changes in amplitude, coefficient of variance (CV), and PPR were calculated by comparing mean values during 5 min intervals specified in each time-course to baseline PPR and CV values. A depression was defined as a significant difference in EPSC, oEPSC, eIPSC or $oIPSC^{FFI}$ amplitude from baseline calculated during the time interval specified in the recording. A shift in $I_{Holding}$ was measured relative to a 3-5-min baseline. Paired or unpaired *t*-tests were used to analyze statistical differences between data sets. Sidak's post-hoc analyses were used for 1-way ANOVAs. Power analyses were performed with preliminary data during the acquisition of each new data set. The sample size obtained from each power analysis calculation was then compared to sample sizes reported in the literature for similar experiments. Errors bars depicted in figures

represent SEM. For all analyses, α was set as 0.05, with P values < α indicating a statistically significant difference.

Supplemental Figures

To discern more clearly the contribution of H_1R and H_2Rs, we superfused a suprathreshold concentration of HA (20 μM) followed by the sequential addition of CTZ and ranitidine **(Fig. S1A)**. While CTZ slightly decreased the HA-induced increase in sAP firing, ranitidine triggered a more substantial reversal **(Fig. S1B).**

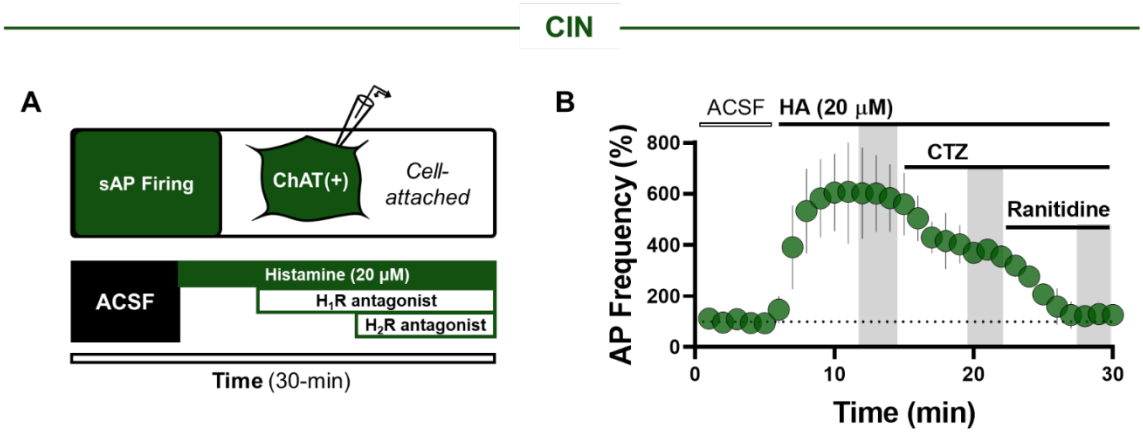

Figure S1. H_2R blockade more significantly reduces the HA-induced increase in sAP firing. (A) Schematic depicting the electrophysiological recording strategy of CINs in cell-attached configuration and drug perfusion schedule. **(B)** Normalized time-course summary depicting the effects of suprathreshold HA (20 μM) following the sequential addition of cetirizine (CTZ, H_1R antagonist) and ranitidine (H_2R antagonist) on sAP firing frequency in CINs (HA: 602.93±176.1%, CTZ: 411.05±37.61%, RANIT: 170.41±40.5%, n=3, CTZ vs. RANIT, p=0.039). Error bars indicate SEM. *p<0.05.

Fig. S2

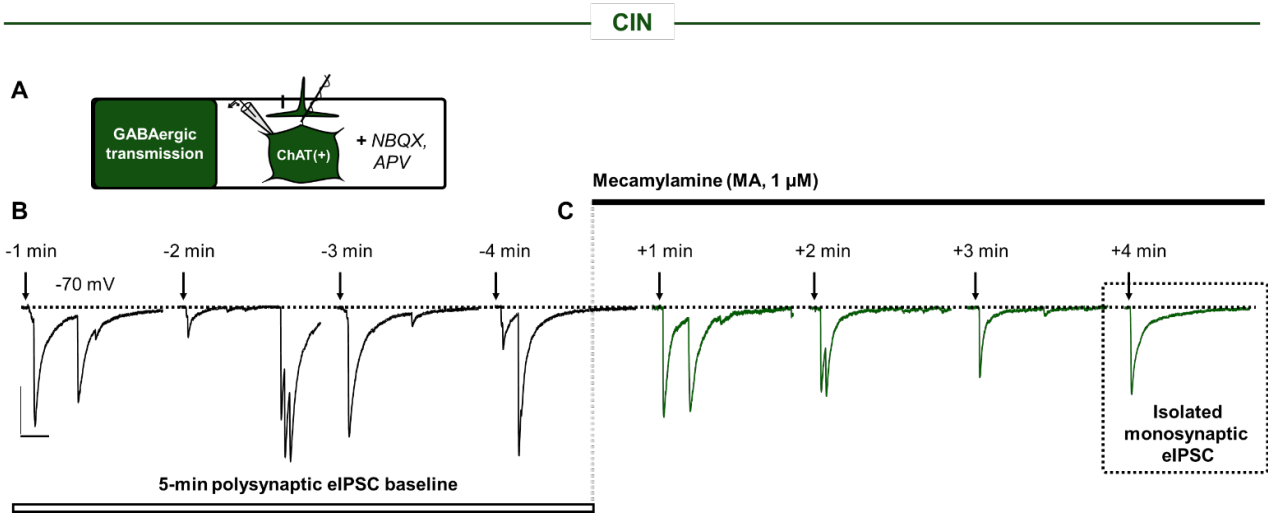

Figure S2. nAChR blockade isolates monosynaptic eIPSCs in NAcSh CINs. (A) Schematic depicting the electrophysiological recording strategy of CINs in whole-cell configuration in the presence of ionotropic glutamate receptor antagonists (NBQX + APV). **(B)** Representative traces depicting polysynaptic, recurrent eIPSCs during a 5-min baseline (black) followed by the gradual resolution of monosynaptic eIPSCs in the presence of broad-spectrum nAChR antagonist, mecamylamine (MA, green). Scale bar: 200-pA/100-ms.

Fig. S3

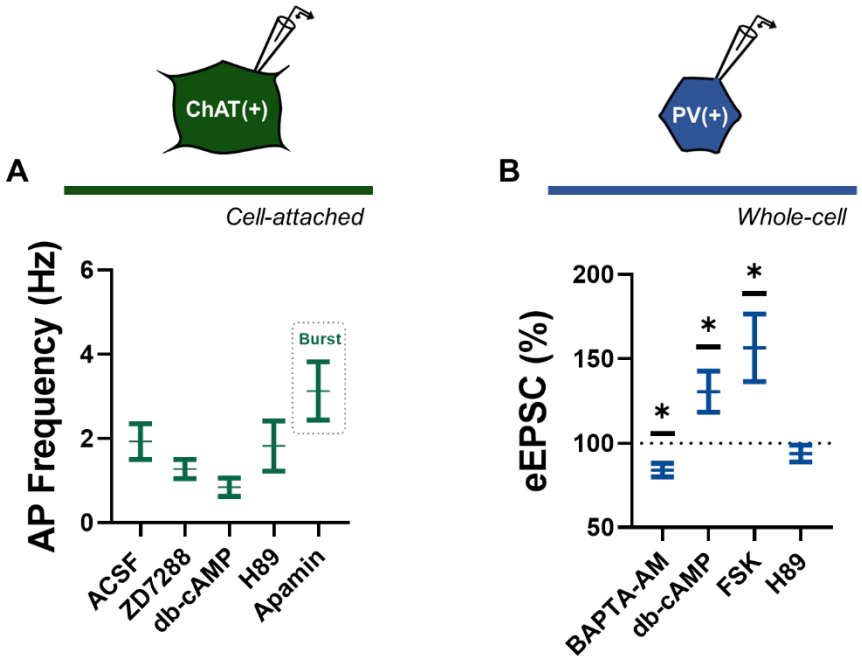

Figure S3. Basal effects of pharmacological manipulations on CIN and PV-INs in the NAcSh.

(A) sAP frequency in CINs measured in cell-attached configuration >10-min following superfusion of each pharmacological agent. ACSF: 1.93±0.42 Hz, n=14 (from Fig. 1L); ZD:1.09±0.26 Hz, n=9; db-cAMP: 0.74±0.21 Hz, n=6; H89: 1.82±0.58 Hz, n=5; apamin: 3.27±0.65 Hz, n=12. ACSF vs. ZD, p=0.659, vs. db-cAMP, p=0.462, vs. H89, p=0.998, vs. apamin, p=0.145, 1-way ANOVA, F(4,42)=2.39, p=0.013). **(B)**. Normalized change in eEPSC amplitude from baseline (ACSF) in PV-INs measured in voltage-clamp configuration: ACSF: 84.07±4.04%, n=4, p=0.029; db-cAMP: 130.5±12.22%, n=5, p=0.033; FSK: 156.6±20.03%, n=6, p=0.037; H89: 93.83±4.93%, n=6, p-0.266. Error bars indicate SEM. *p<0.05.